

The ultraviolet laser from individual ZnO microwire with quadrate cross section

Meng Ding,^{1,2} Dongxu Zhao,^{1,4} Bin Yao,³ Shulin E,¹ Zhen Guo,^{1,2} Ligong Zhang,¹ and Dezhen Shen^{1,*}

¹State Key Laboratory of Luminescence and Applications, Changchun Institute of Optics, Fine Mechanics and Physics, Chinese Academy of Sciences, 3888 Dongnanhu Road, Changchun, 130033, China

²Graduate School of the Chinese Academy of Sciences, Beijing 100049, China

³Department of Physics, Jilin University, Changchun 130023, China

⁴dxzhao2000@yahoo.com.cn

*shendz@ciomp.ac.cn

Abstract: The ZnO microwires with quadrate cross section were synthesized by chemical vapor deposition method. The ultraviolet laser with the Fabry-pérot cavity modes was realized from an individual ZnO microwire. Under the low excitation power densities, the amplified spontaneous emission was observed from the ZnO microwire, while the lasing action was observed under the high excitation power densities. The ZnO microwire exhibited low threshold excitation intensity of 58 kW/cm² and quality factor of 485. The characteristics and possible lasing mechanism were investigated in detail.

©2012 Optical Society of America

OCIS codes: (140.5960) Semiconductor lasers; (140.3610) Lasers, ultraviolet; (140.3380) Laser materials.

References and links

1. Z. K. Tang, G. K. L. Wong, P. Yu, M. Kawasaki, A. Ohtomo, H. Koinuma, and Y. Segawa, "Room-temperature ultraviolet laser emission from self-assembled ZnO microcrystallite thin films," *Appl. Phys. Lett.* **72**(25), 3270–3272 (1998).
2. Z. Guo, H. Zhang, D. X. Zhao, Y. C. Liu, B. Yao, B. H. Li, Z. Z. Zhang, and D. Z. Shen, "The ultralow driven current ultraviolet-blue light-emitting diode based on n-ZnO nanowires/i-polymer/p-GaN heterojunction," *Appl. Phys. Lett.* **97**(17), 173508 (2010).
3. J. B. Baxter and E. S. Aydil, "Nanowire-based dye-sensitized solar cells," *Appl. Phys. Lett.* **86**(5), 053114 (2005).
4. G. P. Wang, S. Chu, N. Zhan, Y. Q. Lin, L. Chernyak, and J. L. Liu, "ZnO homojunction photodiodes based on Sb-doped p-type nanowire array and n-type film for ultraviolet detection," *Appl. Phys. Lett.* **98**(4), 041107 (2011).
5. G. Zhang, X. Shen, and Y. Q. Yang, "Facile Synthesis of Monodisperse Porous ZnO Spheres by a Soluble Starch-Assisted Method and Their Photocatalytic Activity," *J. Phys. Chem. C* **115**(15), 7145–7152 (2011).
6. M. H. Huang, S. Mao, H. Feick, H. Q. Yan, Y. Y. Wu, H. Kind, E. Weber, R. Russo, and P. D. Yang, "Room-Temperature Ultraviolet Nanowire Nanolasers," *Science* **292**(5523), 1897–1899 (2001).
7. D. Wang, H. W. Seo, C. C. Tin, M. J. Bozack, J. R. Williams, M. Park, and Y. Tzeng, "Lasing in whispering gallery mode in ZnO nanonails," *J. Appl. Phys.* **99**(9), 093112 (2006).
8. E. S. Jang, X. Y. Chen, J. H. Won, J. H. Chung, D. J. Jang, Y. W. Kim, and J. H. Choy, "Soft-solution route to ZnO nanowall array with low threshold power density," *Appl. Phys. Lett.* **97**(4), 043109 (2010).
9. D. J. Gargas, M. C. Moore, A. Ni, S. W. Chang, Z. Y. Zhang, S. L. Chuang, and P. Yang, "Whispering Gallery Mode Lasing from Zinc Oxide Hexagonal Nanodisks," *ACS Nano* **4**(6), 3270–3276 (2010).
10. C. Czekalla, C. Sturm, R. Schmidt-Grund, B. Cao, M. Lorenz, and M. Grundmann, "Whispering gallery mode lasing in zinc oxide microwires," *Appl. Phys. Lett.* **92**(24), 241102 (2008).
11. H. Cao, Y. G. Zhao, S. T. Ho, E. W. Seelig, Q. H. Wang, and R. P. H. Chang, "Random Laser Action in Semiconductor Powder," *Phys. Rev. Lett.* **82**(11), 2278–2281 (1999).
12. D. X. Zhao, C. Andrezza, P. Andrezza, J. G. Ma, Y. C. Liu, and D. Z. Shen, "Temperature-dependent growth mode and photoluminescence properties of ZnO nanostructures," *Chem. Phys. Lett.* **399**(4-6), 522–526 (2004).
13. Z. Guo, D. X. Zhao, D. Z. Shen, F. Fang, J. Y. Zhang, and B. H. Li, "Structure and Photoluminescence Properties of Aligned ZnO Nanobolt Arrays," *Cryst. Growth Des.* **7**(11), 2294–2296 (2007).
14. Z. K. Tang, M. Kawasaki, A. Ohtomo, H. Koinuma, and Y. Segawa, "Self-assembled ZnO nano-crystals and exciton lasing at room temperature," *J. Cryst. Growth* **287**(1), 169–179 (2006).

15. Z. W. Pan, Z. R. Dai, and Z. L. Wang, "Nanobelts of semiconducting oxides," *Science* **291**(5510), 1947–1949 (2001).
 16. D. J. Gargas, M. E. Toimil-Molares, and P. D. Yang, "Imaging single ZnO vertical nanowire laser cavities using UV-laser scanning confocal microscopy," *J. Am. Chem. Soc.* **131**(6), 2125–2127 (2009).
 17. M. A. Zimmler, J. M. Bao, F. Capasso, S. Müller, and C. Ronning, "Laser action in nanowires: Observation of the transition from amplified spontaneous emission to laser oscillation," *Appl. Phys. Lett.* **93**(5), 051101–051103 (2008).
 18. R. Chen, B. Ling, X. W. Sun, and H. D. Sun, "Room Temperature Excitonic Whispering Gallery Mode Lasing from High-Quality Hexagonal ZnO Microdisks," *Adv. Mater.* **23**(19), 2199–2204 (2011).
 19. J. C. Johnson, H. Q. Yan, P. D. Yang, and R. J. Saykally, "Optical Cavity Effects in ZnO Nanowire Lasers and Waveguides," *J. Phys. Chem. B* **107**(34), 8816–8828 (2003).
 20. H. Q. Yan, J. Johnson, M. Law, R. R. He, K. Knutsen, J. R. Mckinney, J. Pham, R. Saykally, and P. D. Yang, "ZnO nanoribbon microcavity lasers," *Adv. Mater.* **15**(22), 1907–1911 (2003).
-

1. Introduction

In recent years, short-wavelength semiconductor lasers have been considered as the next generation laser source for wide application prospect in the information technology. Among the wide band-gap semiconductor materials, zinc oxide (ZnO) with a large exciton binding energy (60 meV) and a direct band gap (3.37 eV) has been attracted much more attention for its possible applications in ultraviolet lasers (LDs), light emitting diodes (LEDs), solar cells, detector, photocatalytic and so on [1–5]. Until now, the UV lasing emission has been observed in various ZnO structures, such as ZnO nanowires [6], nanonails [7], nanowalls [8], nanodisks [9] and microwires [10]. There are three kinds of lasing modes to explain the lasing formation. The first one is the random lasing observed usually in ZnO nanopowders [11], where the light is amplified along the closed loop feedback paths caused by the recurrent scattering at crystal boundaries. Because the laser cavity is formed randomly, the laser could be detected in different angles. The second one is the whispering-gallery mode (WGM) lasing observed in ZnO nano/microstructures [7–10], where light travels circularly in the hexagonal structures owing to the total internal reflection at the ZnO/air boundary. Because of this reason, the WGM lasing has the high quality factors (Q factors). Moreover, the WGM lasing is predominantly emitted out at the corners of hexagon. The third one is the Fabry-pérot (F-P) type laser observed in ZnO nanowires [6], where the top and bottom facets of the nanowires serve as two reflecting mirrors, and the F-P type laser has the low threshold.

In this paper, the ultralong ZnO microwires were synthesized by chemical vapor deposition (CVD) method, which was simple, repeated and easy to operate. The side faces of the ZnO microwire with quadrate cross section served as the F-P cavity. Furthermore, the ultraviolet lasing was observed at room temperature from the single ZnO microwire, which showed a low threshold excitation intensity (58 kW/cm²) and the Q factor of 485. The characteristics and possible lasing mechanism were investigated in detail.

2. Experimental details

The ZnO microwires were synthesized via traditional chemical vapor deposition method in a horizontal tube furnace. A mixture of ZnO, graphite powders with a definite weight ratio of 1:1 served as the reactive source. The silicon substrate with about 100 nm thick ZnO film deposited via radio frequency magnetron sputtering method was laid above the source material with a vertical distance of 4 mm. The growth temperature was 1030°C, and the furnace was heated to 1030°C at a speed of 20 °C min⁻¹ from room temperature. After the reaction for 30 min, the furnace was cooled down to the room temperature naturally. The microwires could be observed on the substrate and the inner surface of the boat. During the synthesis process, a constant flow of argon (99.99%) (100 standard cubic centimeters per minute) was introduced into the tube furnace using as the protecting gas.

The morphology of the microwire was characterized by the field emission scanning electron microscopy (FESEM). The photoluminescence (PL) measurement was carried out with a JY-630 micro-Raman spectrometer by using the 325 nm line of a He-Cd laser as the

excitation source. A mode-locked femtosecond Ti:sapphire laser with an optical parametric amplifier (OPA) were performed for the stimulated emission measurement of the ZnO microwire. The femtosecond (pulse width of 120 fs, repetition frequency of 1000 Hz) operating at 350 nm was focused to a spot with the diameter of about 10 μm onto the ZnO microwire. The incidence light is vertical to the surface of the ZnO microwire. The emission signals is collected by a fiber and spectrometer (ACTON spectraPro 2300i) system. The lasing detection direction is shown in Fig. 1(b), the detection angle is angle between pumping light and detection direction, also the direction of pumping light and the sample is fixed and unchanged. All the measurements were performed at room temperature.

3. Results and discussions

A ZnO microwire was chose and fixed its two ends with indium on a cleaned silicon substrate. The typical SEM image of the as-grown single ZnO microwire is clearly shown in Fig. 1(a). The ZnO microwire has four lateral sides, and the average width of ZnO microwires is about 7 μm with the length of 2 cm. The cross section of the ZnO microwire is quadrate, which is clearly shown in the right inset of Fig. 1(a). The reason why the microwires have the quadrate cross section in spite of the hexagonal crystal symmetry of ZnO is deduced. The concentrations of the reaction gases were important to affect the shapes of ZnO nano or micro structures as being reported in our previous work [12, 13]. At low concentrations of zinc vapor, the cross section of ZnO nanostructure is usually a hexagonal shape. But at high concentrations, two-dimensional growth occurs resulting in the cross section shape changing. In our experiments, the growth temperature was beyond 1000 $^{\circ}\text{C}$, which was much higher than the one in the typical carbothermal method [6]. Therefore, the reaction vapor concentration was high, which leded the quadrate cross section presented.

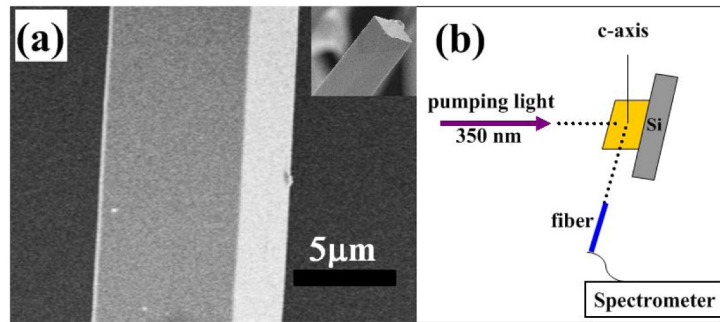


Fig. 1. (a) The SEM image of single ZnO microwire on silicon substrate. The right inset shows the cross section of the ZnO microwire. (b) The schematic diagram for the lasing detection around the ZnO microcavity by moving the fiber.

The PL spectrum of the ZnO microwire excited by using the He-Cd laser was analyzed at room temperature, as shown in the inset of Fig. 2(a). A strong emission peak located at 389 nm could be observed, which is corresponding to the near band edge emission of ZnO. In addition, the defect related visible emission is not observed, which suggests the ZnO microwire is of high crystal quality. In order to explore the possible stimulated emission from the single microwire, the emission spectra at different excitation power densities have been examined. The lasing action in the ZnO microwire during the evolution of the emission spectra with increasing the pump power is observed (as shown in Fig. 2(a)). When the excitation power density is 39 kW/cm^2 , a broad spontaneous emission located at 389.4 nm with the full width at half maximum (FWHM) about 13 nm, which is consistent with the PL measurement using the 325 nm He-Cd laser (as shown in the inset of Fig. 2(a)). With increasing the excitation intensity, the FWHM of the spontaneous emission become much narrower. Once the laser excitation intensity is more than 65 kW/cm^2 , several sharp peaks

with FWHM less than 1 nm appear on a broad spontaneous emission, which suggests a transition process from spontaneous emission to stimulated emission occurs. When the laser excitation density is further increased, the sharp peaks become more and the peak intensity increases dramatically. Under the excitation power density of 181 kW/cm², seven discrete optical modes could be observed located at 390 nm, 391.37 nm, 392.71 nm, 394.05 nm, 395.49 nm, 396.91 nm and 398.31 nm, respectively. Furthermore, with the excitation power intensity increasing, the UV emission shows obvious red-shift, which is accordance with the typical feature of the electron-hole plasma (EHP). The forming reason of EHP emission is mainly that the excitons become unstable and can be ionized easily attributed to the screening effect of Coulomb interaction induced by the large carrier concentration under the high excitation density [14].

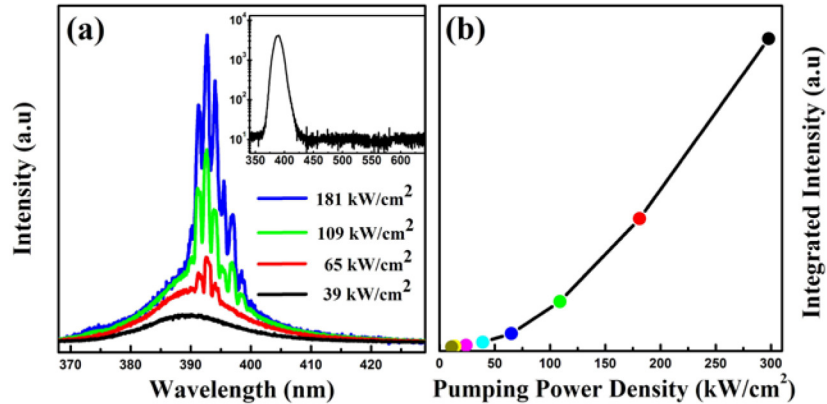


Fig. 2. (a) The emission spectra evolution of individual ZnO microwire with the width of 7 μm under different excitation power intensities with 350 nm (120 fs, 1000 Hz) laser at room temperature. From bottom up, the excitation intensity is 39, 65, 109, 181 kW/cm². The inset is the PL spectrum of the ZnO microwire carried out by using the 325 nm at room temperature. (b) The relationship between the integrated emission intensity and excitation power density on the microwire.

In order to further prove the laser character, the relationship of the integrated emission intensity versus the excitation power density is investigated in Fig. 2(b). The curve shows a nonlinear shape with an obvious threshold of 58 kW/cm². The emission intensity increases slowly below this value. However, when the excitation exceeds 58 kW/cm² the emission intensity increases rapidly, which implies the lasing occurs.

It is well known that the Q factor plays a very important role in describing the laser cavity loss. For a lasing mode, the Q factor can be calculated with the formula:

$$Q = \lambda / \Delta\lambda \quad (1)$$

where λ and $\Delta\lambda$ are the peak wavelength and its FWHM, respectively. In this experiment, the the full width at half maximum of the laser mode is about 0.81 nm at the wavelength of 392.64 nm in Fig. 2(a). Therefore, the corresponding Q factor is about 485 (the pump intensity is 181 kW/cm²).

For the ZnO microstructure there are two different laser cavity modes: WGM and FP. Being considered the values of the threshold and the Q factor, it is deduced that the most probable lasing mechanism should be F-P laser cavity. For the F-P cavity, the quadrature structure plays an important role in producing lasing. The laser cavity is formed by the opposite side planes of the single ZnO microwire. Based on our previous work on ZnO nanostructure [12] and Prof. Zhonglin Wang's work on ZnO nanobelts [15], the growth direction of ZnO microstructure was along (002) direction. So the side surfaces,

($\bar{2}\bar{1}\bar{1}0$) or ($0\bar{1}\bar{1}0$) facets, served as the F-P mirrors. The modes spacing could be calculated by the following formula [16]:

$$\Delta\lambda = \lambda^2 / [2L(n - \lambda dn/d\lambda)] \quad (2)$$

where n is the relative refractive index of about 2.4 and L is the effective cavity length (the width of ZnO microwire is about 7 μm observed in the SEM image), the $dn/d\lambda$ is the Sellmeier first-order dispersion relation (the value of $dn/d\lambda$ is -0.015 nm^{-1} at 390 nm) [17], respectively. The calculated $\Delta\lambda$ is 1.32 nm according to the above equation, which is consistent with the experimentally observed mode space of 1.34 nm in Fig. 2(a). The Q factor for F-P cavity can be determined by the following equation:

$$Q = 2\pi nL / \lambda(1-R) \quad (3)$$

where R is the reflectivity at the ZnO/air boundary ($R \sim 15.5\%$). From this equation the Q factor is calculated as 320, which is lower than the value obtained in the experiment. Compared with the normal F-P cavity, the quadrate-shaped cross section of the ZnO microwire could improve the confinement of the emissions in the cavity, which results in the enhancement of the Q factor. While the Q factor of laser generated from in WGM cavity is higher than from FP cavity, it is mainly because that the light wave propagates circularly in the inner walls due to multiple total internal reflection at the ZnO/air boundary, the total internal reflection makes the resonator nearly free from mirror losses, which is as high as 3300 [18].

The threshold condition for the laser oscillation could be given as the following equations [19,20]:

$$\Gamma g_{\text{th}} = \alpha_w + \alpha_m, \quad \alpha_m = (2L)^{-1} \ln(R_1 R_2)^{-1} \quad (4)$$

where Γ is the confinement factor, g_{th} is the material gain, α_w is the waveguide loss, α_m accounts for the losses at the end facets (the mirror losses). For ZnO nanowires, the cavity length is much smaller and the reflection coefficient is small, $\alpha_m \gg \alpha_w$, so the waveguide loss can be neglected. But in microwires, the cavity was formed by the side facets, which is much smaller than the length of microwire, the waveguide loss should be large and considered in our obtained ZnO microwire laser. Therefore, the threshold in our experiment is a little higher than the values obtained in ZnO nanowires.

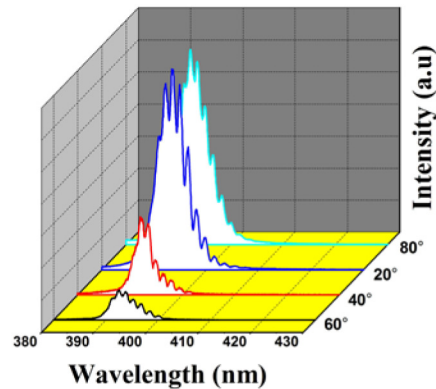


Fig. 3. The emission spectra of individual ZnO microwire with the width of 7 μm at different detection angle under the excitation power intensities of 181 kW/cm^2 at room temperature.

To observe the directivity of the laser, the emission spectra of the ZnO microwire with different detection angles (the angle between pumping light and detection direction) under the

excitation power intensities of 181 kW/cm^2 was measured at room temperature (as shown in Fig. 3). A broad emission band accompanying with some sharp peaks could be observed for the detection angles at 20° , 40° , 60° and 80° , respectively. The peak positions for the sharp emission peaks are irregular.

4. Summary

In conclusion, ZnO microwires have been fabricated by chemical vapor deposition method. The UV lasing from the individual ZnO microwire was obtained, in which the lasing threshold was 58 kW/cm^2 , and the Q factor was 485. By analyzing the lasing characteristics, the laser emission modes were in agreement well with the F-P cavity. It was deduced the quadrate-shaped cross section of the ZnO microwire could increase the optical confinement, which induced the Q factor measured is higher than the theoretical calculations value in our experiment.

Acknowledgments

This work is supported by National Basic Research Program of China (973 Program) under Grant Nos. 2011CB302006, 2011CB302004, the Knowledge Innovation Program of the Chinese Academy of Sciences under Grant No. KJCX2-YW-W25.